

DESIGN OF THE SUPERCONDUCTING LINAC FOR SARAF

C. Madec, N. Bazin, L. Boudjaoui, R. Cubizolles, G. Ferrand, B. Gastineau, Ph. Hardy, C. Pes, N. Pichoff, N. Sellami, Ph. Bredy, CEA, Saclay, France
P. Bertrand, GANIL, Caen, France

Abstract

CEA is committed to delivering a Medium Energy Beam Transfer line and a superconducting linac (SCL) [1] for SARAF accelerator in order to accelerate 5mA beam of either protons from 1.3 MeV to 35 MeV or deuterons from 2.6 MeV to 40.1 MeV. The SCL consists 4 cryomodules equipped with warm diagnostics. The first two identical cryomodules host 6 half-wave resonator (HWR) low beta cavities ($\beta = 0.091$), 176 MHz. As the last two identical welcome 7 HWR high-beta cavities ($\beta = 0.181$), 176 MHz. The beam is focused through the superconducting solenoids located between cavities and housing steering coils. A Beam Position Monitor is placed upstream each solenoid. A diagnostic box containing a beam profiler, a bunch length monitor and a vacuum pump will be inserted between 2 consecutive cryomodules. The HWR cavities, the solenoid package, the cryomodules and the warm sections are being designed. These studies will be presented in this contribution.

CAVITIES DESIGN

RF Design of the Half Wave Resonators

Two different half wave cavity resonators are being studied for the SARAF Linac project, for two different β_{opt} parameters: 0.091 and 0.181 respectively referred as low and high beta cavities. The frequency of the cavity corresponds to the frequency of the bunches : 176 MHz. These cavities are designed for a 5 mA continuous beam current.

To reach the high accelerating voltage per cavity, the electromagnetic design was carefully optimized:

- The peak surface electric field has to be minimized to reduce field emission; 35 MV/m is considered as a reasonable peak electric field;
- The peak magnetic field was set to 70 mT in order to be lower than the 180 mT transition magnetic field from superconducting state to normal;
- The dissipated power on the walls of the cavity must be minimized to reduce the cryogenic cost.

Specific cavity geometrical parameters have been used for the optimization. They are shown on Figure 1 and defined as:

- R_{in} : radius of the central drift tube element;
- R_{ext} : outer radius of the cavity;
- R_b : small radius of the torus;
- Z_c : thickness of the drift tube;

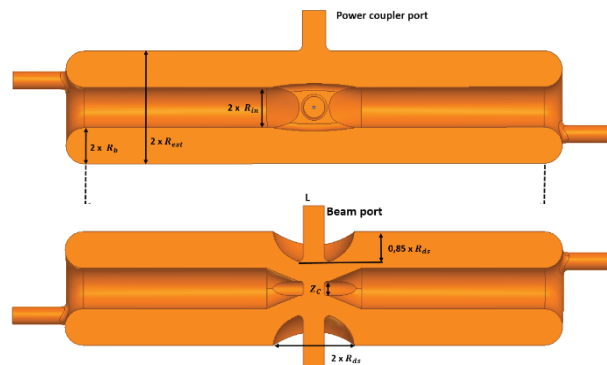


Figure 1: Main parameters of the cavities. Top diagram: cut perpendicular to the beam axis. Bottom diagram: cut perpendicular to the coupler antenna axis.

- R_{ds} : radius of the beam nozzle;
- L : length of the cavity.

The optimization has to take into account constraints imposed by the beam dynamic studies. The cavity flange-to-flange distance is defined as 280 mm and 410 mm for the low and high beta cavities respectively. When considering the flange dimensions and the helium tank design, this defines a maximum value for R_{ext} as 95 mm and 160 mm for the low and high beta cavities respectively.

The cavities will be placed vertically, thus, the liquid helium will flow through the drift tube in order to avoid helium bubbles and local heat. A channel of 10mm diameter was considered as a minimum for ensuring a comfortable helium flow at 4 K. We chose to manufacture the drift tube by digital machining to reduce the welding risk in this part of the cavity that shows very high electric field. These defines the minimum value of R_{in} to 34 mm. Simulations were carried out with the Ansys HFSS software. The results of the optimization are detailed in Table 1. The table shows that magnetic and electric field peak limits, 70 mT and 35 MV/m are respected by this design, at the nominal acceleration field.

Mechanical Design of the Low Beta HWR and its Helium Tank

The nominal value of Q_{ext} ($1.21 \cdot 10^6$) sets the cavity 3 dB bandwidth at nominal beam current to 289 Hz for the low beta HWR. The amplitude of the He pressure fluctuations in the 4.45 K cryostat is expected to be +/-5 mBar. This implies that He pressure sensitivity df/dP in the order of 10 to 5 Hz/mbar has to be reached in order to limit the extra RF power consumption.

The mechanical design of the HWR and helium tank consists in determining bulk parts and the thickness of the Niobium and Titanium sheets.

Simulations were provided with Ansys Mechanical software, with the nutshell approximation for Niobium and Titanium sheets.

Table 1: RF Performances of the Cavities

| Parameter | Low Beta | High Beta |
|----------------------------|-------------------|-------------------|
| β opt | 0.0911 | 0.181 |
| E_{acc} (MV/m) | 6.5 | 7.5 |
| E_{pk}/E_{acc} | 5.04 | 4.35 |
| E_{pk} (MV/m) | 32.8 | 32.6 |
| B_{pk}/E_{acc} (mT/MV.m) | 10.3 | 7.60 |
| B_{pk} (mT) | 66.6 | 57.1 |
| R/Q (Ω) | 166.2 | 277.9 |
| G (Ω) | 33.1 | 53.1 |
| Q_0 at $R_s = 20n\Omega$ | $1.66 \cdot 10^9$ | $2.65 \cdot 10^9$ |
| P_{diss} at R_s (W) | 3.70 | 7.19 |

The stresses remain acceptable in the cavity and helium tank, while the thickness of the Niobium sheets is higher than 3 mm everywhere. According to the simulations, three parts will be manufactured from bulk niobium: extremity torus, drift tubes and beam nozzle (see Figure 2). The deformation at 2 bar is described in Figure 3. The resulting Helium bath sensitivity was estimated with the cavity perturbation method: 4.3 Hz/mbar. The bandwidth of the low-beta cavity being 289 Hz, this does not exceed $1/10^{th}$ of the bandwidth for a variation of ± 5 mbar. The reflected power, in these conditions is lower than 0.5%.

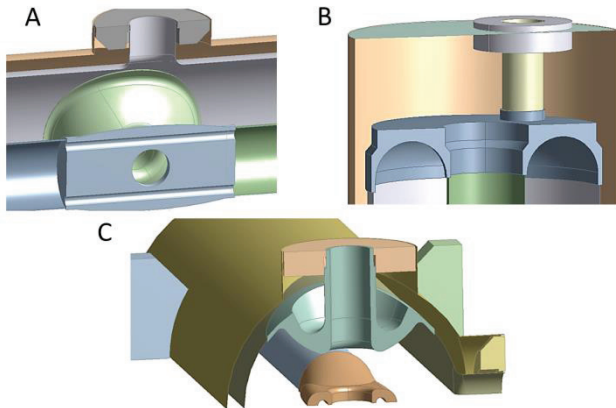


Figure 2: Considered bulk parts for HWR cavity. (A) Drift tube. (B) Extremity torus. (C) Beam nozzle.

RF POWER COUPLER DESIGN

RF couplers have to transfer to the beam 4.8 kW for the low- β section and 11.5 kW for the high- β section. Assuming a maximal extra power of 40% required for mismatches and cavity field control, the power coupler,

E: Static Structural
Total Deformation
Type: Total Deformation
Unit: mm
Time: 1

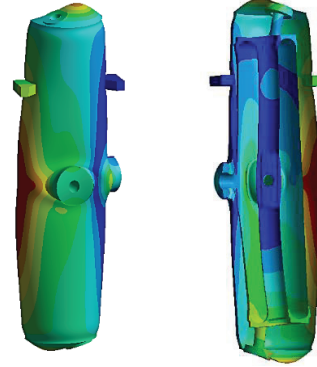
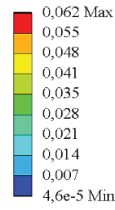


Figure 3: Deformation under a 0.2 MPa pressure of the niobium cavity and its helium tank. Deformation amplification factor: 1500.

identical for both cavities, is designed, with margins, for 20 kW RF power.

The coupling is electrical, with a copper antenna located at the mid-plane of the cavity, orthogonal to the beam axis. At this location, the magnetic field vanishes, preventing extra losses on the normal conducting antenna. The coaxial line connected to the cavity flange has an aperture of 40 mm. The design is based on a single warm window, which is brazed in a 3 1/8" EIA coaxial line. The area around the ceramic disc of the window (thickness 10 mm) is optimized to achieve a low reflection coefficient (< -30 dB). A thin Titanium Nitride (TiN) layer is deposited on the ceramic in order to reduce the secondary electron emission yield. The horizontal portion of the antenna has to be short (smaller than 300 mm) in order to keep a small overall width of the cryostat (smaller than 1.5 m).

The optimal external quality factor Q_{ext} are $1.21 \cdot 10^6$ and $1.66 \cdot 10^6$ for the low- β section and high- β section, respectively. Given the moderate powers to supply, the couplers have a fixed coupling, thus simplifying the fabrication. The coupling factors for both low- β and high- β sections are adjusted by only changing the antenna length. The RF studies (with Ansys HFSS) show that an error of ± 1.5 mm on the antenna length increases the reflected power to only 5%. Consequently, the adjustment of the antenna length is not critical.

A permanent cooling of pure clean air is used to keep the ceramic window at ambient temperature and to prevent from condensation. Both inner and outer conductors are cooled by conduction. The external conductor inside the cryostat, from the ceramic to the cavity flange, is a copper plated stainless steel tube and has a thermal intercept at 60 K to minimize the heat flux at 4.45 K. The input of the coupler is directly connected to the standard 3 1/8" EIA rigid line coming from the RF power source without RF transition. Figure 4 shows the design.

The coupler is connected to the cryomodule with a bellow (not represented in Figure 4, connected to the cryomodule flange) that provides flexibility during cool-down of the cryomodule.

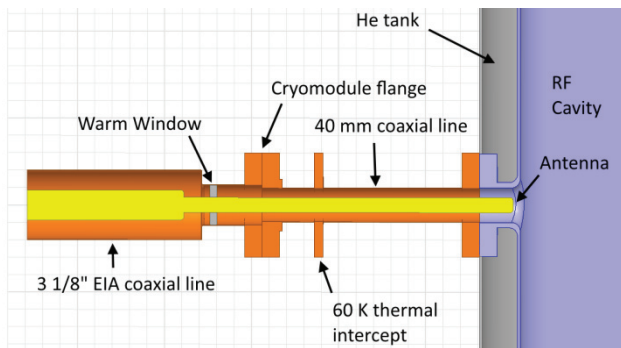


Figure 4: Diagram of the coupler.

SOLENOIDE PACKAGE DESIGN

The solenoid package includes the main solenoid, the shielding coils and the dipole coils to provide beam focalization and steering corrections in both horizontal and vertical planes. Each Solenoid Package includes also two bellows and a Beam Position Monitor. To reduce the fringe field at the superconducting cavities, two Helmholtz coils, coaxial with the main solenoid, in series and in opposition, will ensure its active shielding. The whole set has been optimized to get a fringe field lower than 20 mT, at 140 mm from the solenoid center. With a 400 A/mm² engineering current density, the integrated on-axis square field is higher than 2.9 T².m. The nominal current, not yet defined, will be between 200 and 400 A. Main parameters of this Solenoid Package are summarized in the following Table 2, while the Figure 5 illustrates the magnetic design of this package.

Table 2: Main Solenoid Parameters

| Parameter | Nominal | Design | Units |
|--|---------|--------|-------------------|
| Beam aperture | 40 | 40 | mm |
| Flange-to-flange (m) | 340 | 340 | mm |
| Maximum magnetic field By on beam axis | 5.8 | 6.4 | T |
| $\int By^2 dy$ | >2.9 | 3.5 | T ² .m |
| Integrated steering field | 7 | 8 | mT.m |

CRYOMODULE DESIGN

The cryomodules are of the two types: low-beta cryomodules (CM1 & CM2) which house seven $\beta=0.091$ half-wave resonators and six focusing solenoids, and high beta cryomodules (CM3 & CM4) which house seven $\beta=0.181$ half-wave resonators and four focusing solenoids. The valves boxes to distribute the cryogenic liquids to the cryomodules and the warm section are included in the description.

While the accelerator lattice and by consequence the total length differ between the two kinds of cryomodule enough similarities exist such as the main principles in the design could be used with minor modifications.

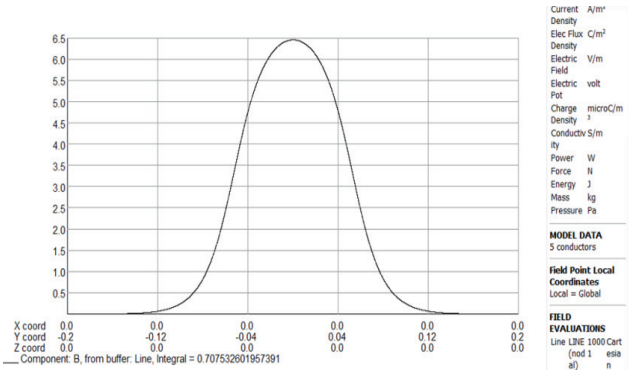
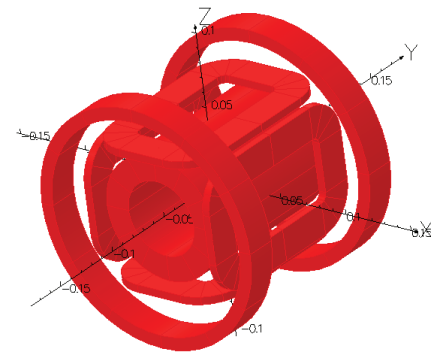


Figure 5: Magnetic design of the Solenoid Package, and the resulting magnetic field profile on its axis.

Cryomodule Conceptual Design

The SARAF-Phase 2 cryomodule design is built upon past CEA experience with IFMIF cryomodules.

The cold mass – i.e. the cavity string and the cryogenic circuit – will be supported by a titanium frame. Copper braids will be connected between this frame and the cryogenic. The distribution of the braids will be optimized in order to limit the thermal contraction during the cooling down [2].

Because of the thermal shrinking of the frame during the cool down of the cryomodule it is not possible to attach directly the cavities and the solenoids on this one in order to be compatible with the couplers which are in interface with the vacuum vessel. To leave the cavities and solenoids longitudinal position independent from the titanium frame, C-shaped elements with needle rollers similar to the ones presented in [3] are used. Each cavity and solenoid is fixed on an invar rod which is attached to the frame in its centre. Because of the low thermal expansion coefficient of invar (0.4 mm/m between ambient temperature and liquid Helium temperature to compare to 1.5 mm/m for titanium), this invar rod fixture determines the longitudinal positions of the couplers.

The components of the cavity string – cavities with their power couplers, solenoids and warm/cold transitions with beam valves will be assembled on the frame in clean room using the principle described in [4].

In order to reduce the risk of magnetization parts due to the solenoids and steerers operation, nonmagnetic materials will be used when possible for the components close to the magnetic area of the superconducting cavities. For example, homemade bearings with ceramic needle

and brass cage will be used for the C-shaped elements instead of the off-the-shelf rollers originally intended to be used [5, 6].

One requirement by SNRC, is to have a cryomodule width less than 1.78 m for the displacement in the corridor along the accelerator during installation and maintenance. This constraint has been taken into account for the cryomodule design.

The experience gained on IFMIF design allows us to propose the top-loaded box cryomodule: the whole cold mass as well as the thermal shield is supported by the top plate of the vacuum vessel. This setup simplifies the assembly process and most important the alignment of the cavity string.

The conceptual design is depicted in Figure 6. The cryogenics circuit is made of two inlet manifolds supplying helium to the cavities and the solenoids. The pipes will be designed to limit the imbalance of the Helium supply for each component. A phase separator is placed at the top of the cold mass where liquid level and pressure will be regulated for the cavity and solenoid tanks located just below. A thermal shield intercepts the radiative heat loads from the parts at room temperature. All the parts with one end at room temperature and the other end at liquid helium temperature (cold mass supports, cables for sensors and actuators, current lead packages, etc...) will be heat sunk on the thermal shield. A warm magnetic shield, attached to the inner surface of the vacuum vessel, protects the superconducting cavities against the Earth magnetic field.

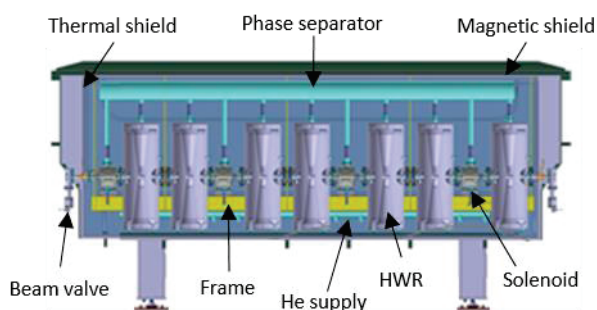


Figure 6: Conceptual design of the high-beta cryomodule (CM3 & CM4).

Cryogenics and Valve Box

Based on the same design as SARAF-Phase 1, the four cryomodules will be considered as cold baths filled in parallel with saturated liquid helium at 4.45 K (0.125 MPa abs.). These vessels will be supplied with liquid helium at 4.45 K by using a supercritical helium. This helium, whose pressure is around 0.5 MPa and temperature 5.5 K, will be supplied by a cryoplant through a primary cryogenic transfer line (SNRC deliverable) to four valves boxes (CEA deliverable) –one per cryomodule – which contains a Joule-Thomson valve necessary to expand the supercritical helium to get liquid helium at 4.45 K and all the other cold valves necessary

to cool down and warm-up the cryomodules. The principle of the cryogenic system is shown in Figure 7.

Four helium circuits coming from the main transfer line have to be connected to the inlet of the valve boxes which will be located in the service corridor: the inlet supercritical helium, the return helium gas, and inlet and outlet for gaseous helium necessary to cool the thermal shield (around 70 K). To connect the valves boxes to the cryomodule, the lines shall pass through the concrete wall separating the service corridor to the accelerator corridor. The type of line is not defined yet: a single transfer line similar to the main transfer line with a bellow to ease the assembly to the cryomodule, or several flexible lines with bayonet connections. The choice will be a trade-off between heat loads and possible compensation of the errors in the positioning of the elements.

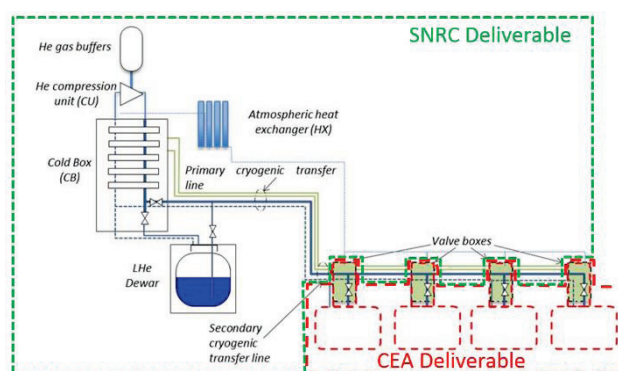


Figure 7: Principle of the cryogenic system.

Warm Sections

The distance between consecutive cryomodules is around 307 mm and is filled with a warm section made of a 50 mm diameter beam tube with bellows at each end. In the middle of the warm section is located a diagnostic box with two perpendicular DN100 to install a Bunch Extension Monitor and one DN63 port for connecting a turbo molecular pump.

Vacuum simulations were performed to compare the pressure profile along the beam axis when pumping through the warm section or using a specific line connected to two central cavities as for the IFMIF cryomodule [7]. Results are presented in Figure 8. The small diameter of the beam pipe (Ø50 mm for the warm sections, Ø40 mm for the solenoids, Ø36 mm for the low-beta cavities and Ø40 mm for the high-beta cavities) limits the conductance when pumping through the warm sections, reducing the pumping speed from 75 l/s to 15 l/s. Pumping through the HPR ports of two central cavities provides a better vacuum with a pressure profile along the beam axis more homogeneous.

Measurements of the bunch longitudinal shape of the beam is fundamental for the optimization and control of the LINAC beam parameter. Although not completely validated by beam dynamics simulations, the installation of BEM (Bunch Extension Monitor) is considered. A good candidate for such a device could be the BEMs developed at GANIL for the SPIRAL2 accelerator. The

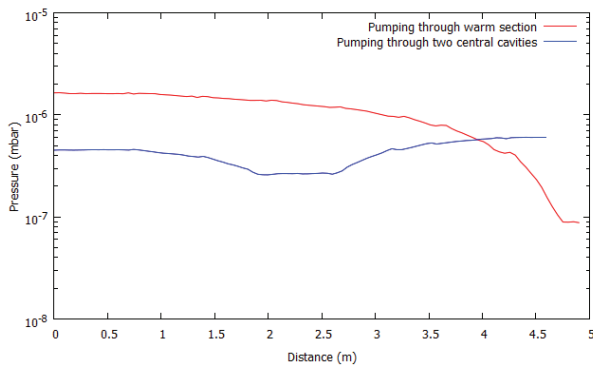


Figure 8: Pressure profile along the beam axis for the two studied setups.

principle of a BEM is based on an X-ray detector registering the photons emitted by a Tungsten wire in interaction with the beam. The photons interact with MCP channels and produce secondary emission electrons due to the photoelectric effect (Figure 9).

The BEM shall be UHV compatible since the LINAC is operating at 10^{-8} mbar and they shall be particle free in order to prevent cavity pollution. A prototype was successfully tested with an Oxygen beam at GANIL, and all the BEM [8] are being installed at SPIRAL2 to be used in 2016.

As for SPIRAL2, realistic tests should be required as soon as a SARAF operational cryomodule is available, in order to check that the X-ray background is compatible with such a BEM.

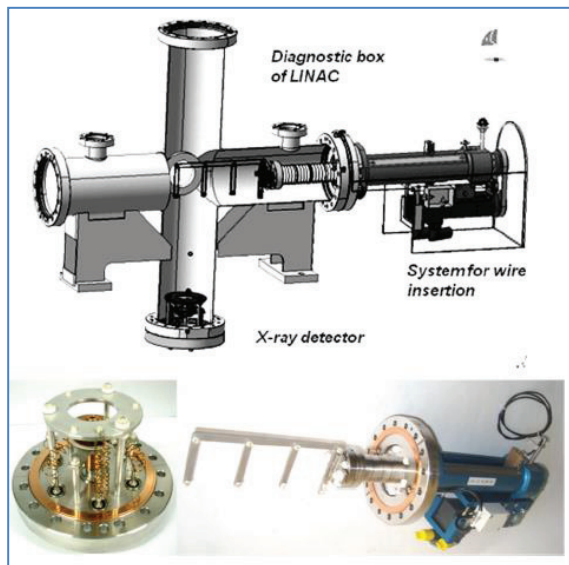


Figure 9: SIRAL2 BEM box and view of BEM components.

REFERENCES

- [1] N. Pichoff, "The SARAF-LINAC project for SARAF Phase 2", THPF005, IPAC2015, Richmond.
- [2] N. Bazin, "Thermo-mechanical study of the support frame for the IFMIF cavity string", THPB114, these proceedings, SRF 2015, Whistler, Canada.
- [3] C. Pagani, "Advances in cryomodule design and new approaches", SRF 1999, Berlin, Germany.
- [4] N. Bazin et al., "Development of a test bench to prepare the assembly of the IFMIF LIPAC cavity string", TUPB107, these proceedings, SRF 2015, Whistler, Canada.
- [5] N. Bazin et al., "Magnetic aspect of the IFMIF cryomodule", TTC meeting, Tsukuba, Japan, December 2014.
- [6] H. Dzitko et al., "Design and manufacturing status of the IFMIF-LIPAc SRF Linac", IPAC 2015, Richmond, USA, THPF006.
- [7] N. Bazin et al., "Vacuum study of the cavity string for the IFMIF-LIPAc cryomodule", IPAC 2013, Shanghai, China, THPFI003.
- [8] R. Rovenko, "J.L. Vignet, SPIRAL2 Bunch Extension Monitor", LINAC 2014, Geneva, Switzerland, September 2014.